Origin of Au nanostructures on tungsten surface carbides

A. Varykhalov, O. Rader, and W. Gudat
BESSY, Albert-Einstein-Str. 15, D-12489 Berlin, Germany

(Received 16 June 2007; revised manuscript received 16 October 2007; published 14 January 2008)

The template-assisted self-organization of Au deposited on surface carbides W(110)/C-$R(15\times12)$ and W(110)/C-$R(15\times3)$ is investigated by means of scanning tunneling microscopy, low energy electron diffraction, and photoelectron spectroscopy. The existence of two principally different ways of self-organization of Au nanostructures is revealed on each of the substrates. The *room temperature deposition* results in the growth of Au nanoclusters controlled by the potential profile of the carbidic nanomesh. The Au clusters are aligned along the surface carbide and appear uniform but geometrically different on the different carbides. In particular, they are *one monolayer high* when grown on the $R(15\times12)$ structure and *two monolayers high* on the $R(15\times3)$ structure. Subsequent *annealing* of the sample at 900–1000 K produces a rearrangement of Au adatoms toward a one-dimensionally patterned overlayer with nanowirelike reconstruction which is identical on a both W(110)/C-$R(15\times12)$ and W(110)/C-$R(15\times3)$ and no longer aligned along the surface carbide but along the [001] direction of the W. This delivers strong evidence that self-organization at elevated temperature is driven by chemical Au-W interaction. Additional support for this explanation is found in photoemission spectra from the valence band and the W 4*f* core level. The W 4*f* shows a large core-level shift of +440 meV which exists neither for the bare surface carbides $R(15\times12)$ and $R(15\times3)$, nor for Au on pure W(110), nor for Au deposited on the surface carbides without annealing.

DOI: 10.1103/PhysRevB.77.035412 PACS number(s): 68.37.Ef, 79.60.Jv, 81.16.Dn, 81.16.Rf

I. INTRODUCTION

The feasibility of surface reconstructions to control self-assembly of adsorbed atoms and molecules toward nanostructures with reduced dimensionality has been confirmed by many reports published so far. Among the most prominent examples are "magic" clusters on Si(111)-(7×7),[1] magnetic dots[2] and a fullerene nanomesh[3] grown on vicinal Au(111), and chains of Au atoms on stepped Si.[4] Such systems are used as miniature quantum labs on which a wide range of quantum-size effects can be studied and the limits of future nanoelectronic devices can be explored.[5]

A very specific role in the family of templates supporting self-organization is played by the tungsten surface carbide W(110)/C-$R(15\times3)$,[6,7] the ability of which to control self-assembly of adsorbed materials with markedly contrasting structural and electronic properties can be referred to as *universal*. For instance, it can trap fullerene molecules and force them into a two-dimensional molecular gas, which, in turn, condensates into "magic" clusters stabilized by weak van der Waals interactions.[8] Another example of self-organization on W(110)/C-$R(15\times3)$ is annealing-assisted assembly of Au nanostripes in which the lateral confinement of electrons was evidenced.[9] Most recently, these Au nanostripes were proven to be themselves a suitable template for self-assembled magnetic nanowires.[10]

Within the present paper, we continue our research on tungsten surface carbides and extend it to the temperature-assisted self-organization of Au on the second intrinsic (albeit metastable[11]) superstructure of carbon on W(110), i.e., W(110)/C-$R(15\times12)$. By means of scanning tunneling microscopy (STM), low energy electron diffraction (LEED), and photoelectron spectroscopy (PES), we demonstrate the identity of Au nanowires produced on the two carbidic templates $R(15\times12)$ and $R(15\times3)$ and conclude on a carbon-mediated chemical interaction between Au and W atoms as the origin of the observed self-assembly.

This is a very interesting finding about the high-temperature formation of one-dimensional (1D) Au nanostructures with possibly important consequences. The effect described does not depend on the exact geometry of the carbon superstructure adsorbed at the W surface but is rather controlled by the chemical properties of the constituents of the self-assembled compound. This is a key prerequisite for implementation of this technique in mass production of Au-derived nanostructured materials. As we will demonstrate below, the observed self-organization is sensitive neither to the crystal properties of the tungsten surface carbide nor to the precise conditions of the chemical reaction, meaning that the material combination Au/C/W may due to this flexibility be highly feasible for large-scale fabrication of nanostructured functional materials such as catalysts, devices, and magnetic storage media.

We also conducted STM and PES characterizations of Au as deposited at room temperature on W(110)/C-$R(15\times12)$ and W(110)/C-$R(15\times3)$. In contrast to the 1D reconstruction which appears after annealing, Au grows at $T=300$ K as uniform nanoclusters. Apparently, the nucleation of Au adatoms is at this temperature directly mediated by the potential profile of the carbidic nanomesh and not by the chemical interaction to the underlying W substrate. Particularly interesting are Au clusters nucleated on W(110)/C-$R(15\times3)$: being 2 ML (monolayer) thick and less than 2 nm wide, they are a potential low-temperature catalyst, as will be pointed out.

II. EXPERIMENT

Experiments were performed with an Omicron VT STM operated at room temperature. We used electrochemically

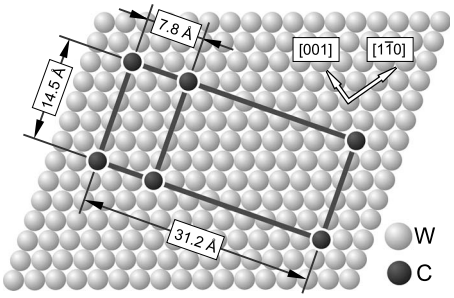

FIG. 1. Periodicity and lattice orientation of two surface carbides on W(110). The unit cell of the metastable phase W(110)/C-$R(15\times12)$ corresponds to four unit cells of the stable carbide W(110)/C-$R(15\times3)$.

etched polycrystalline W tips treated *in situ* by annealing. Photoelectron measurements were performed with a SPECS Phoibos 150 hemispherical analyzer at 80 meV total energy and 1° angular resolution. The undulator beamline UE112 at BESSY was used as source of linearly polarized light. Base pressure during experiments was below 2×10^{-10} mbar.

The W(110) sample was initially cleaned as described elsewhere.[7,12] The stable phase of the surface carbide on W(110) is usually prepared by annealing the sample in a partial pressure of C_3H_6 (1×10^{-6} mbar) at 750–800 K. A subsequent flash of the crystal at ~2300 K results in a perfect carbidic superstructure evidenced by a sharp $R(15\times3)$ LEED pattern [Fig. 3(b)] and the well known meanderlike morphology in the STM image [Fig. 2(b)].

For the preparation of the $R(15\times12)$ phase, referred to as metastable by Baudoing and Stern,[11] we have developed a procedure which is remarkably easy as compared to the method commonly used. Instead of transforming the $R(15\times3)$ into $R(15\times12)$ by treating the sample at 2600 K, the metastable phase can be achieved in the same way as described above but the substrate temperature must be elevated to 1000–1100 K during vapor deposition of propylene. Formation of the $R(15\times12)$ nanomesh can be evidenced by a complicated rhombohedral LEED pattern accompanied by multiple spots of lower intensity [Fig.3(a)]. STM images of this system (not atomically resolved) demonstrate the typical pattern of periodically arranged larger and smaller spots [Fig. 2(a)], in full agreement with earlier studies.[6]

Location and lateral orientation of both carbidic superlattices on W(110) are compared in Fig. 1.[6,11] In matrix notation (Park-Malden), the $R(15\times12)$ and $R(15\times3)$ superstructures are defined as

$$\begin{pmatrix} 5 & 0 \\ -4 & 12 \end{pmatrix} \quad \text{and} \quad \begin{pmatrix} 5 & 0 \\ -1 & 3 \end{pmatrix},$$

respectively. The carbidic matrices are rotated relative to basis vectors of W(110) by 14°. The exact atomic structures of $R(15\times12)$ and, to a lesser extent, $R(15\times3)$ are not yet established in detail. The main obstacle to this are p_z orbitals of carbon adatoms, which are directed perpendicular to the surface and which interfere with the STM tip and cause a strong distance-dependent variation of the image morphology.[7,13] As a result, this largely invalidates the information about exact atomic locations.

III. RESULTS AND DISCUSSION

A. Room temperature self-assembly

We begin with Au deposited on the surface carbides at room temperature. This phase will be further referred to as *room temperature self-assembly*. The STM investigation reveals that for coverages below 1 ML, Au nucleates as small nanoclusters, the dimension, orientation, and lateral arrangement of which are determined by the geometry of the carbon superstructure on W(110). Figures 2(c) and 2(d) display large-scale STM images for $R(15\times12)$ and $R(15\times3)$, respectively, with ~0.2 ML of deposited Au. The formation of uniform clusters is apparent. On W(110)/C-$R(15\times12)$, these nanoclusters even tend to arrange themselves into chains aligned along a high symmetry direction of the carbidic template. STM images taken at enhanced magnification [Figs. 2(e) and 2(f)] reveal that the geometry of Au clusters is different on $R(15\times12)$ and $R(15\times3)$.

On the metastable $R(15\times12)$ phase, the nanoclusters appear laterally less uniform and, in average, slightly wider than on $R(15\times3)$ [Fig. 2(g)]. Diagrams presenting the size distribution of Au clusters are shown in Figs. 2(h) and 2(i). A reliable reference for the cluster widths is ensured by the simultaneous observation of the template periodicity in the STM data [see inset just below Fig. 2(f)]. The strict limitation of nanocluster dimensions in one direction (perpendicular to the carbide rows) confirms the hypothesis about the existence of carbon-induced 1D relaxation of the W lattice supported in Ref. 7 by photoemission from surface electronic states of W(110). From the diagrams, one obtains principal widths of observed Au clusters as 1.7–2.6 nm on $R(15\times12)$ and 1.4–1.8 nm on $R(15\times3)$.

Comprising these observations, we conclude that room-temperature self-assembly of Au is explicitly mediated by the potential profile of the surface carbide.

The key difference between Au nanoclusters on the two carbides is their thickness. Line sections S_1 and S_2 in Fig. 2(g) disclose that on W(110)/C-$R(15\times3)$, Au nucleates in 2 ML-thick clusters, in contrast to nanoclusters on W(110)/C-$R(15\times12)$ which are 1 ML thick. This difference in the thickness is obviously related to the mobility of Au atoms adsorbed on the two different carbides. As was demonstrated by means of simple kinetic models for Au on oxide surfaces, formation of three-dimensional islands is generally favorable since they are more stable thermodynamically.[14,15] Tendencies toward a two-dimensional growth regime are determined by the interaction between Au adatoms and the substrate. This means for the present case that the carbon superstructure with the larger lateral periodicity interacts stronglier with the Au. This also corresponds well to indications that Au quantum dots are trapped in the $R(15\times12)$ carbide matrix upon high-temperature self-assembly (see further below).

The remarkable combination of double layer thickness and small lateral dimensions (<2 nm) renders Au clusters on

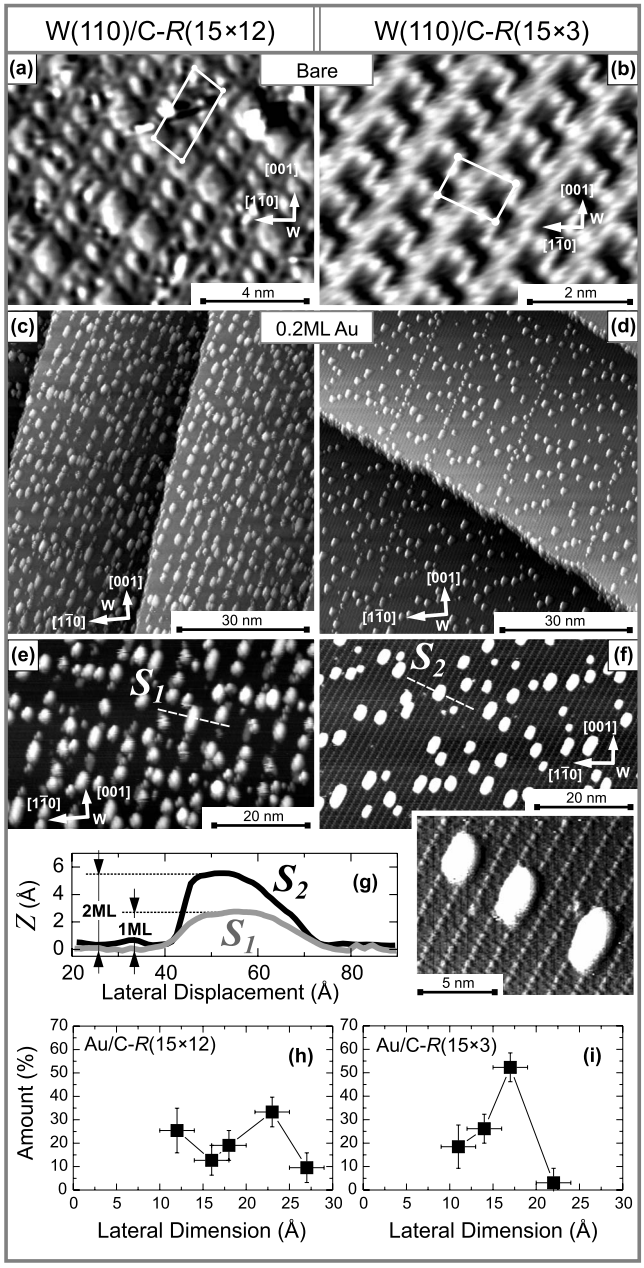

FIG. 2. Characterization of room temperature self-assembly by STM. [(a) and (b)] STM images of bare surface carbides (a) W(110)/C-$R(15\times12)$ and (b) W(110)/C-$R(15\times3)$ obtained at "slow" feedback (representing predominantly the modulation of the tunneling current). [(c) and (d)] Large-scale STM images of 0.2 ML Au deposited on (c) $R(15\times12)$ and (d) $R(15\times3)$ at room temperature. [(e) and (f)] Insight into the Au nucleation on (e) $R(15\times12)$ and (f) $R(15\times3)$. The inset displays a fine-scale image of Au nanoclusters on $R(15\times3)$ with clearly visible alignment to the substrate. (g) Characteristic topography profile of Au clusters on the two carbides. [(h) and (i)] Size distribution of Au clusters on (h) $R(15\times12)$ and (i) $R(15\times3)$.

the stable carbide W(110)/C-$R(15\times3)$ highly relevant for catalysis. In fact, an enhanced catalytic activity has been observed with Au islands of 2 ML height on an oxidic substrate.[16–18] There are basically two contesting theories intending to explain these interesting catalytic properties. While one theory invokes quantum-size effects in the 2 ML Au islands, the other one postulates the creation of a $Au^{\delta+}$ state caused by oxygen in the substrate. Apparently, the present template for the 2 ML Au islands does not contain any oxygen so that an investigation of the catalytic activity for Au on W(110)/C-$R(15\times3)$ could help solving this important issue.

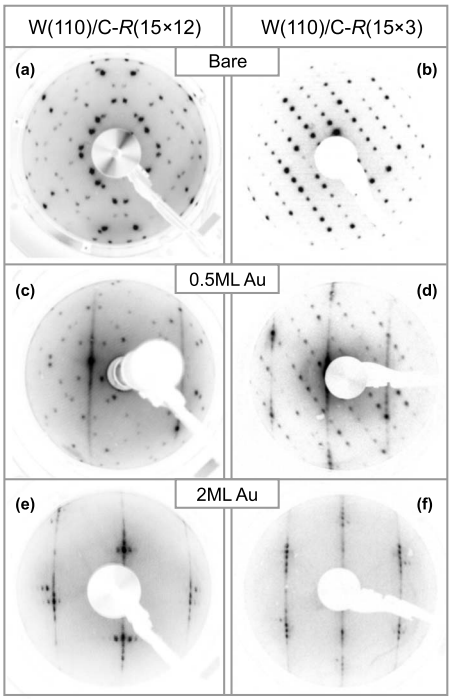

FIG. 3. Characterization of high-temperature self-assembly by LEED. [(a) and (b)] Patterns from bare surface carbides (a) $R(15\times12)$ and (b) $R(15\times3)$. [(c) and (d)] Nanowires self-organized from 0.5 ML of Au on (c) $R(15\times12)$ and (d) $R(15\times3)$ after annealing at 1000 K. [(e) and (f)] High-temperature self-organization of 2-ML-thick Au. For thick Au films annealed on $R(15\times12)$, a certain tendency toward two dimensionality is visible.

B. High-temperature self-assembly

A second type of Au nanostructures, which is one dimensional, appears when "as deposited" Au is annealed at 900–1000 K. Formation of the nanowirelike structure (further referred as *high-temperature self-assembly*) is observed for up to four nominal Au monolayers. We have already studied this phenomenon on W(110)/C-$R(15\times3)$ (see Refs. 9 and 10), and in the present report, we compare results of those previous experiments with high temperature self-assembly on the metastable phase W(110)/C-$R(15\times12)$. The created nanowires appear to be identical on both carbides as evidenced by LEED and STM measurements.

LEED photographs taken from $R(15\times12)$ and $R(15\times3)$ with Au coverage <1 ML show a characteristic 1D pattern after annealing [Figs. 3(c) and 3(d), respectively]. Submonolayer coverage of Au allows for the observation of electron diffraction from the Au wires and the carbidic template si-

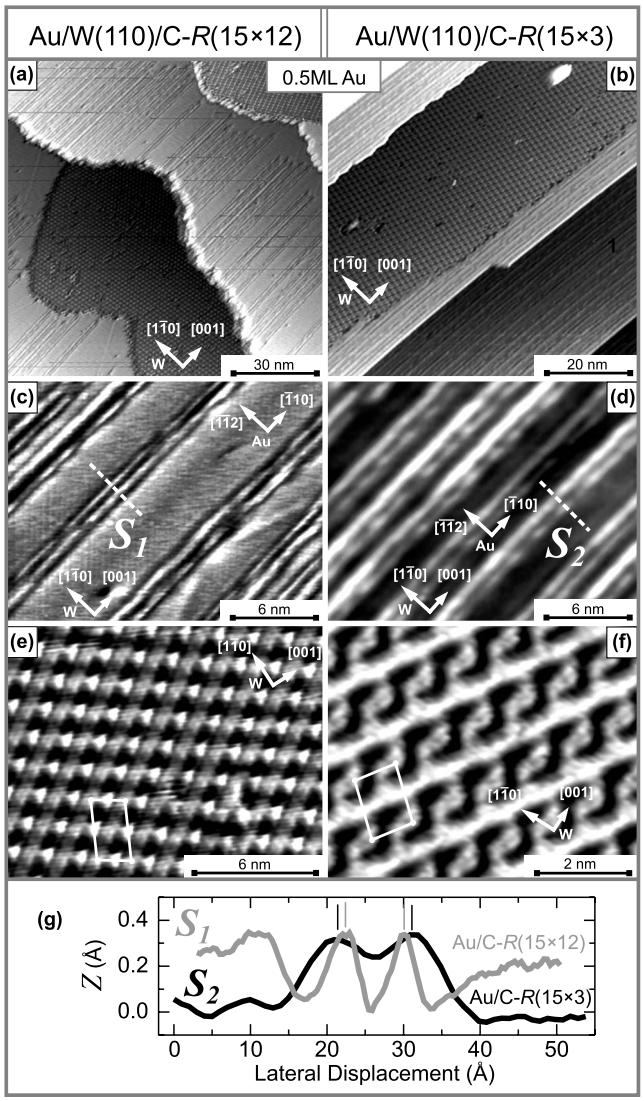

FIG. 4. Characterization of high-temperature self-assembly by STM. [(a) and (b)] Large scale STM images of surface carbides (a) $R(15\times12)$ and (b) $R(15\times3)$ with 0.5 ML Au annealed at 1000 K. [(c) and (d)] STM images of nanowirelike patterned Au islands on (c) $R(15\times12)$ and (d) $R(15\times3)$. [(e) and (f)] fine-scale STM images of uncovered substrate areas between the patterned Au islands. An array of nanodots is observed in the case of metastable carbide $R(15\times12)$. (g) Topography profiles across Au wires.

multaneously. This clarifies orientation and lattice geometry of the one-dimensional Au nanostructure. As the main diffraction spots from Au in the LEED patterns shown in Figs. 3(c)–3(f) are aligned relative to the (1,0) spots of W(110)-$p(1\times1)$, one concludes that Au atoms are laterally arranged as Au(111). This is also confirmed by our recent atomically resolved STM experiment.[10]

More structural information is delivered by STM measurements which are reported in Fig. 4. Comparison of the STM images taken for 0.5 ML Au annealed on the $R(15\times12)$ and $R(15\times3)$ structures [Figs. 4(a) and 4(b), respectively] discloses similar dynamics of the self-organization on both templates. Adsorbed Au coalesces into large islands where the nanowires appear as 1D surface reconstruction. A fine-scale STM characterization of the surface of Au islands is reported in Figs. 4(c) and 4(d). Nanowires show up in pairs, the width of each wire is about 1 nm. Transversal line scans $S_{1,2}$ displayed in Fig. 4(g) prove the geometrical identity of the nanowirelike reconstruction on both carbides. The difference in the appearance of Au wires in Figs. 4(c) and 4(d) is due to different geometries of STM tips used in the experiment.

Between the islands of Au one sees superstructures. Their periodicity and the fact that they exist in two orientational domains are identical to the original $R(15\times12)$ and $R(15\times3)$ templates. This suggests that these regions are open areas of the original carbidized substrates. Figures 4(e) and 4(f) show fine-scale STM images of these areas. There might be, however, a principal difference in the chemical composition between the bare surface carbide $R(15\times12)$ [Fig. 2(a)] and $R(15\times12)$ uncovered by Au after annealing [Fig. 4(e)]. While the STM characterization of uncovered $R(15\times3)$ [Fig. 4(f)] does not indicate any difference as compared to the freshly prepared $R(15\times3)$ [Fig. 2(b)], in the analogous situation for W(110)/C-$R(15\times12)$, we observe drastic changes. Testing this system with different tips reveals a significant asymmetry in the topography of almost every surface unit cell due to spatial variation in the local density of states or in the surface work function. As a result, the $R(15\times12)$ template appears in STM as an array of perfectly arranged nanodots [Fig. 4(e)]. Albeit a careful local spectroscopic characterization is required to reach a decisive conclusion about the nature of these dots, we intend to identify them as Au atoms (or clusters) trapped in the $R(15\times12)$ matrix of carbon. Such scenario is highly probable if one considers the geometry of the metastable surface carbide, in which the largely nonuniform atomic arrangement of carbon[6] across the unit cell should cause significant variation in the surface potential. In such case, Au adatoms require more energy to diffuse over the lattice until potential wells are sealed by trapped clusters. We consider these nanodots an exciting object for further research.

Taking the results of LEED and STM measurements together, we can make the remarkable conclusion that *geometry and orientation* of the fabricated nanowires are *insensitive* to the structural phase of the carbide used as template. In fact, high temperature self-assembly appears absolutely identical on $R(15\times12)$ and $R(15\times3)$. To find the key to this puzzle, we have tested both systems by photoemission from the valence band and the chemically sensitive W $4f$ core level.

C. Photoemission

Consistently with the results of LEED and STM measurements, PES shows that electronic structure and chemical compositions of Au nanowires are nearly identical on both templates $R(15\times12)$ and $R(15\times3)$. Only minor differences in the photoelectron spectra of W $4f$ could be revealed (Fig. 5). The substrate core level was probed at $h\nu=70$ eV through approximately two nominal monolayers of Au. Photoemis-

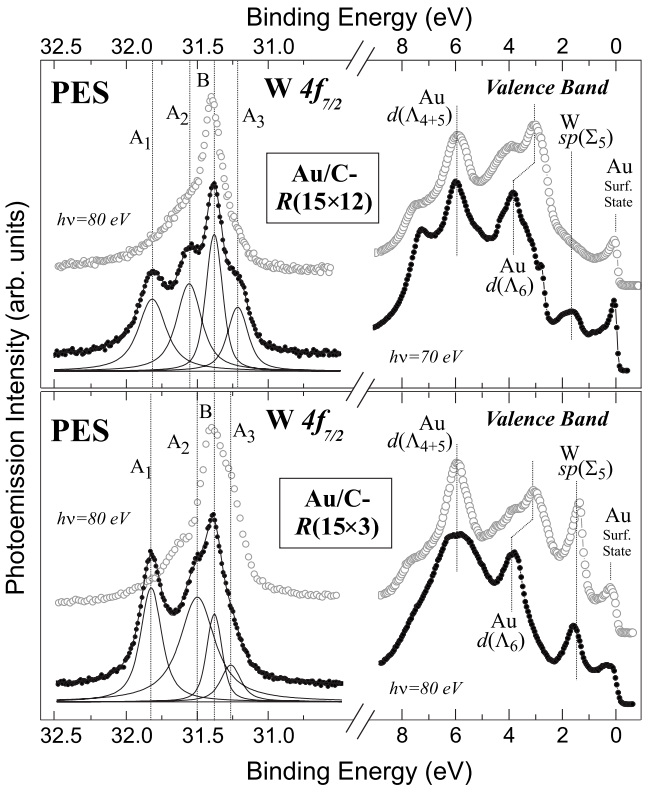

FIG. 5. Photoemission study of Au nanostructures on surface carbides $R(15\times12)$ (upper panel) and $R(15\times3)$ (lower panel). Open circles denote measurements with as deposited Au (room temperature self-assembly) and filled circles represent spectra measured after annealing (high-temperature self-assembly). For the high-temperature phase, the spectral composition of W $4f$ core level is complicated (peaks $A_{1\text{-}3}$) but identical for both carbides. Symbol B denotes emission from bulk. The effect of chemical interaction between Au and W can also be seen in photoemission from the valence band.

sion from the valence band was measured with a coverage of 1 ML Au.

For as deposited Au, we observe no changes in the shape of W $4f$ (open circles in Fig. 5) as compared to the spectra of the bare surface carbides.[7] This additionally confirms that room temperature self-assembly of Au nanoclusters is mediated by the potential profile of the carbidized template. However, after annealing and formation of the Au wires, a number of new spectral components $A_{1\text{-}3}$ appear (filled circles in Fig. 5). In both cases of $R(15\times12)$ and $R(15\times3)$, they have nearly the same binding energy and only deviate in intensities. This low sensitivity of the W $4f$ core level to the structural arrangement of carbon on W(110) leads us to conclude that the observed core-level shifts are due to chemical interaction between Au adatoms and W substrate. This appears to be interaction activated by chemisorbed carbon which perturbs the W lattice. Each chemical shift $A_{1\text{-}3}$ corresponds to a particular environment of W atoms to Au, with only three possible principal configurations. A comparative study of core-level photoemission for Au on clean W(110) (not reported here) reveals only negligible traces of these peaks which can be attributed to Au-W interaction at the sites of defects. The change in the chemical state of Au atoms upon self-organization is additionally confirmed by photoemission of the W $4f$ core level which we discussed previously.[10]

That components $A_{1\text{-}3}$ in W $4f$ photoemission are caused by the chemical environment is additionally confirmed by the analysis of final-state contributions. Attentive employment of the deconvolution routine allows for a comparative evaluation of core-hole lifetimes for peaks $A_{1\text{-}3}$. The quasiparticle lifetime is largely dependent on the peculiarities of the screening process,[19] hence the sensitivity of the linewidth to the chemical environment. We have found the following Lorentzian widths[20] for $A_{1\text{-}3}$ chemical shifts: in the case of $R(15\times3)$, 130, 260, and 120 meV, respectively, and in the case of $R(15\times12)$, 190, 160, and 110 meV, respectively. The bulk-derived photoemission B provides a linewidth of 65 meV for both substrates being fully consistent with earlier studies.[21] The linewidths of chemically shifted peaks $A_{1\text{-}3}$ are markedly larger than those of the W $4f$ (110)-surface-derived component (84 meV),[21] meaning efficient photohole screening due to the presence of sp electrons of Au. Lifetimes of components A_1 and A_2 as compared for both carbides manifest, however, significant differences. While the environment of W atoms to embedded Au can be considered for both substrates identical due to indentical chemical shifts $A_{1\text{-}3}$, variation of the screening can be attributed to different structural arrangements of carbon surrounding the Au species embedded into the surface compound.

The effect of the charge redistribution can also be noticed in photoemission from the valence band which is shown in Fig. 5 as well. Spectra were taken from Au/C-$R(15\times12)$ and Au/C-$R(15\times3)$ before and after annealing (open and filled circles, respectively) for an emission angle close to the surface normal. The peak near the Fermi energy is a prominent Au(111) surface state which develops at the cluster surface. The apparent intensity variation is due to a small difference in emission angle. A substantial redistribution of the density of states is seen between 3 and 4 eV binding energies. Remarkably, this effect is sensitive to the symmetry properties of d-band wave functions.[22,23] As Fig. 5 shows, the redistribution of charge involves only d-states which belong to the Λ_6 symmetry group, meaning hybridization with W d bands of $\Sigma_{5(2)}$ symmetry.[24] d states at 6 eV (Λ_4,Λ_5) remain unaffected by high temperature self-assembly.

To sum up, we conclude that the *origin* of one-dimensional Au nanostructures self-organized at high temperature on carbidized W(110) is a *chemical interaction* between Au and W atoms. It possibly results in surface alloying. Anisotropic hybridization between d states of Au and W switches the atomic arrangement at the interface to one of the three favorable local configurations and induces significant strain into the Au film. This stress propagates through an up to 4-ML-thick Au overlayer[10] and is released in the form of a nanowirelike 1D reconstruction on its surface. This explanation is consistent with the fact that the orientation of nanowires is close to [001] of W as observed by STM and LEED and not aligned to high symmetry directions of the carbon superstructure [in the case of $R(15\times3)$]. Carbon acts only as mediator which perturbs the W(110) substrate and allows for Au-W interaction. A similar scenario

can be expected in the case of any other adsorbate which bonds to W strongly enough to induce a deformation of the W lattice. In the framework of this concept the trapped Au nanodots [Fig. 4(e)] can be understood as periodically arranged sites of surface-alloy formation which are stable on the $R(15\times12)$ template even in the absence of a continuous Au overlayer.

IV. SUMMARY

In summary, we have compared self-organization of Au on W(110)/C-$R(15\times12)$ (metastable) and W(110)/C-$R(15\times3)$ (stable) surface carbides. It was shown that room temperature self-assembly of Au toward well uniform nanoclusters is governed by the potential profile of carbon superstructures. In contrast, high-temperature self-assembly results in the formation of a Au film with nanowirelike reconstruction, the geometry, and orientation of which are identical for both templates and therefore insensitive to the structural arrangement of carbon on the W(110) surface. Based on the results of our photoemission investigation, a carbon-mediated chemical interaction between Au and W is suggested as origin of one-dimensional high-temperature self-assembly. The geometry of Au nanostructures on carbidized W(110) makes them highly relevant for enhanced catalytic activity.

[1] H. H. Chang, M. Y. Lai, J. H. Wei, C. M. Wei, and Y. L. Wang, Phys. Rev. Lett. **92**, 066103 (2004).
[2] N. Weiss, T. Cren, M. Epple, S. Rusponi, G. Baudot, S. Rohart, A. Tejeda, V. Repain, S. Rousset, P. Ohresser, F. Scheurer, P. Bencok, and H. Brune, Phys. Rev. Lett. **95**, 157204 (2005).
[3] N. Neel, J. Kroger, and R. Berndt, Adv. Mater. (Weinheim, Ger.) **18**, 174 (2006).
[4] I. K. Robinson, P. A. Bennett, and F. J. Himpsel, Phys. Rev. Lett. **88**, 096104 (2002).
[5] J. N. Crain, J. L. McChesney, Fan Zheng, M. C. Gallagher, P. C. Snijders, M. Bissen, C. Gundelach, S. C. Erwin, and F. J. Himpsel, Phys. Rev. B **69**, 125401 (2004).
[6] M. Bode, R. Pascal, and R. Wiesendanger, Surf. Sci. **344**, 185 (1995).
[7] A. Varykhalov, O. Rader, and W. Gudat, Phys. Rev. B **72**, 115440 (2005).
[8] A. Varykhalov, W. Gudat, V. K. Adamchuk, and O. Rader, Phys. Rev. B **73**, 241404(R) (2006).
[9] A. Varykhalov, O. Rader, and W. Gudat, Phys. Rev. B **72**, 241404(R) (2005).
[10] A. Varykhalov, C. Biswas, W. Gudat, and O. Rader, Phys. Rev. B **74**, 195420 (2006).
[11] R. Baudoing and R. M. Stern, Surf. Sci. **10**, 392 (1968).
[12] A. M. Shikin, O. Rader, G. V. Prudnikova, V. K. Adamchuk, and W. Gudat, Phys. Rev. B **65**, 075403 (2002).
[13] M. Bode, R. Pascal, and R. Wiesendanger, Z. Phys. B: Condens. Matter **101**, 103 (1996).
[14] S. C. Parker, A. W. Grant, V. A. Bondize, and C. T. Campbell, Surf. Sci. **441**, 10 (1999).
[15] C. T. Campbell, S. C. Parker, and D. E. Starr, Science **298**, 811 (2002).
[16] M. Valden, X. Lai, and D. W. Goodman, Science **281**, 1647 (1998).
[17] M. S. Chen and D. W. Goodman, Catal. Today **111**, 22 (2006).
[18] D. W. Goodman, Catal. Lett. **99**, 1 (2005).
[19] *Electron Spectroscopy: Theory, Techniques and Applications*, edited by C. R. Brundle and A. D. Baker (Academic, New York, 1978).
[20] To deconvolute the W $4f_{7/2}$ spectra, Voigt functions have been used. Best fit results were achieved for Gaussian functions fixed at full width at half maximum (FWHM)=100 meV [for $R(15\times3)$] and FWHM=90 meV [for $R(15\times12)$] consistently with the energy resolution during experiments. The asymmetry parameter was neglected.
[21] D. M. Riffe, G. K. Wertheim, P. H. Citrin, and D. N. E. Buchanan, Phys. Scr. **41**, 1009 (1990); D. M. Riffe, G. K. Wertheim, and P. H. Citrin, Phys. Rev. Lett. **63**, 1976 (1989).
[22] H. Eckardt, L. Fritsche, and J. Noffke, J. Phys. F: Met. Phys. **14**, 97 (1984).
[23] R. Courths, H.-G. Zimmer, A. Goldmann, and H. Saalfeld, Phys. Rev. B **34**, 3577 (1986).
[24] R. H. Gaylord and S. D. Kevan, Phys. Rev. B **36**, 9337 (1987).